Mammalian Genome 13, 259–267 (2002).
DOI: 10.1007/s00335-001-3054-2

Mammalian Genome
Incorporating *Mouse Genome*

Genetic and molecular control of folate-homocysteine metabolism in mutant mice

Sheila Ernest,[1] Benedicte Christensen,[2]* Brian M. Gilfix,[2] Orval A. Mamer,[3] Angela Hosack,[2] Mitchell Rodier,[2] Clemencia Colmenares,[4] James McGrath,[5] Allen Bale,[5] Rudi Balling,[6] David Sankoff,[7] David S. Rosenblatt,[8] Joseph H. Nadeau[1]

[1]Department of Genetics, Case Western Reserve University School of Medicine; Center for Computational Genomics, Case Western Reserve University; and Center for Human Genetics, University Hospitals of Cleveland, Cleveland, Ohio, USA
[2]Departments of Human Genetics and Medicine, McGill University, Montreal, Quebec, Canada
[3]Department of Medicine, Royal Victoria Hospital, Montreal, Quebec, Canada
[4]Department of Cancer Biology, Lerner Research Institute, Cleveland Clinic Foundation, Cleveland, Ohio, USA
[5]Genetics Department, Yale University School of Medicine, New Haven, Connecticut, USA
[6]Institut für Säugetiergenetik für Umwelt und Gesundheit, GSF Forschungszentrum, Neuherberg, Germany
[7]Centre de recherches mathématiques, Université de Montréal, Québec, Canada
[8]Departments of Human Genetics, Medicine, Pediatrics, and Biology, McGill University, Montreal, Quebec, Canada

Received: 20 June 2001 / Accepted: 1 February 2002

Abstract. Hyperhomocysteinemia adversely affects fundamental aspects of fetal development, adulthood, and aging, but the role of elevated homocysteine levels in these birth defects and adult diseases remains unclear. Mouse models are valuable for investigating the causes and consequences of hyperhomocysteinemia. We used a phenotype-based approach to identify mouse mutants for studying the relation between single gene mutations, homocysteine levels as a measure of the status of homocysteine metabolism, and gene expression profiles as a way to assess the impact of protein deficiency in mutant mice on steady-state transcription levels of genes in the folate-homocysteine pathways. These mutants were selected based on their propensity to produce phenotypes that are reminiscent of those associated with anomalies in folate-homocysteine metabolism in humans. We report identification of new, single-gene mouse models of homocysteinemia and characterization of their molecular and physiological impact on folate-homocysteine metabolism. Mutations in several genes involved in the hedgehog and WNT signal transduction pathways, as well as a gene involved in lipid metabolism, resulted in elevated homocysteine levels and altered expression profiles of folate-homocysteine metabolism genes. These results begin to unravel the complex relations between elevation of a single amino acid in the blood and the diverse birth defects and adult diseases associated with hyperhomocysteinemia.

Various birth defects and adult diseases occur more frequently when blood levels of homocysteine (HCY), a sulfur-containing amino acid, exceed 16 μmol/L (Kang et al. 1992). Normal human HCY blood levels usually range from 4.9 to 11.7 μmol/L (Pietrzik and Bronstrup 1997). Hyperhomocysteinemia (significantly elevated homocysteine levels) occurs at a frequency of 5% in the general population (Hankey and Eikelboom 2000). It is an independent risk factor for neural tube defects (NTDs; MRC Vitamin Research Group 1991; Steegers-Theunissen et al. 1991) and is also associated with colon, breast, ovarian, and pancreatic cancer (Mayer et al. 1996), Alzheimer disease (Clarke et al. 1998; Joosten et al. 1997; Miller 1999), and with certain treatments for Parkinson disease (Muller et al. 1999). The variety of birth defects and adult diseases associated with elevated HCY levels is striking. It is not obvious how elevated levels of a single amino acid and its metabolites could adversely affect so many organs, tissues, and physiological processes. Moreover, it is unclear whether elevated HCY is itself pathogenic or simply a disease marker.

Homocysteine is remethylated through the trans-methylation pathway or irreversibly catabolized through the trans-sulfuration pathway (Mudd et al. 2001; Fig. 1). It contributes directly to methylation of DNA, proteins, and lipids; it contributes indirectly to glucose metabolism and the citric acid cycle. Homocysteine metabolism is also tightly linked to folate metabolism (Fig. 2), which is the major pool of single carbon units. Both pathways participate in purine and pyrimidine biosynthesis and amino acid metabolism (alanine, glycine, and serine; Rosenblatt and Fenton 2001). Regulation of the folate and homocysteine pathways is complex and, because of their inter-relatedness, it is difficult to predict the biochemical and phenotypic consequences of inhibiting particular steps (Kisliuk 1999).

Mutations in MTHFR (methylenetetrahydrofolate reductase; Christensen et al. 1999; Kang et al. 1991; Kanwar et al. 1976), CBS (cystathionine β-synthase; Boers et al. 1985; Mudd et al. 1964), MTR (homocysteine:methionine methyltransferase, also known as methionine synthase; Gulati et al. 1996; Leclerc et al. 1996), and MTRR (methionine synthase reductase) are also associated with hyperhomocysteinemia (Leclerc et al. 1998). More importantly, the cumulative effect of these various mutations does not readily account for the frequency or diversity of these birth defects and adult diseases. Other sources of variation include mutant alleles that have more subtle effects in these genes (Goyette et al. 1996; van der Put et al. 1998), mutations in other genes in folate-homocysteine metabolism, or perhaps mutations in genes in other developmental and physiological pathways.

As a first step towards understanding the genetic and molecular controls of homocysteine levels, a panel of mutant mice was characterized for serum homocysteine levels and for hepatic expression profiles of most genes in the folate-homocysteine pathways, with a comparable number of other genes as controls. An important part of the experimental design was to characterize HCY levels and gene expression in mice with single-gene mutations that have phe-

* *Present address* for B. Christensen: Department of Medical Genetics, Ulleval University Hospital, Oslo, Norway.

Correspondence to: J. Nadeau at Genetics Department, Case Western Reserve University School of Medicine, 10900 Euclid Ave. (regular mail) 2109 Adelbert Road (express mail) Cleveland, Ohio 44106, USA; E-mail: jhn4@po.cwru.edu

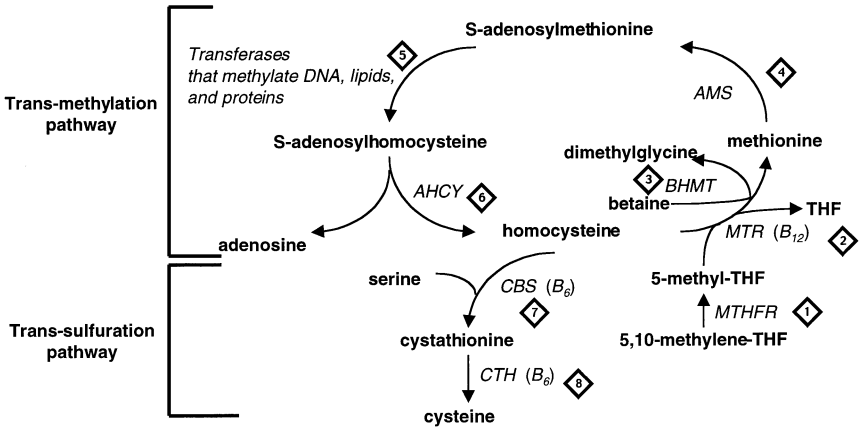

Fig. 1. Homocysteine metabolism. Homocysteine is metabolized through the remethylation or the trans-sulfuration pathways. Remethylation occurs when methionine synthase [MTR, step 2] transfers a methyl group from methyltetrahydrofolate (CH3-THF) to homocysteine, or when betaine-homocysteine methyltransferase [BHMT, step 3] transfers a methyl group from betaine to homocysteine. Transsulfuration occurs by condensation of serine and homocysteine through the action of cystathionine β-synthase [CBS, step 7] to form cystathionine. Labels: Methylene-THF reductase [MTHFR, step 1]; homcysteine:methionine methyltransferase or methionine synthase [MTR, step 2]; betaine-homocysteine methyltransferase [BHMT, step 3]; S-adenosylmethionine synthase [AMS, step 4]; methyltransferases [step 5]; S-adenosylhomocysteine hydrolase [AHCY, step 6]; cystathionine β-synthase [CBS, step 7]; cystathionine γ-Iyase [CTH, step 8]; vitamins B6 and B12.

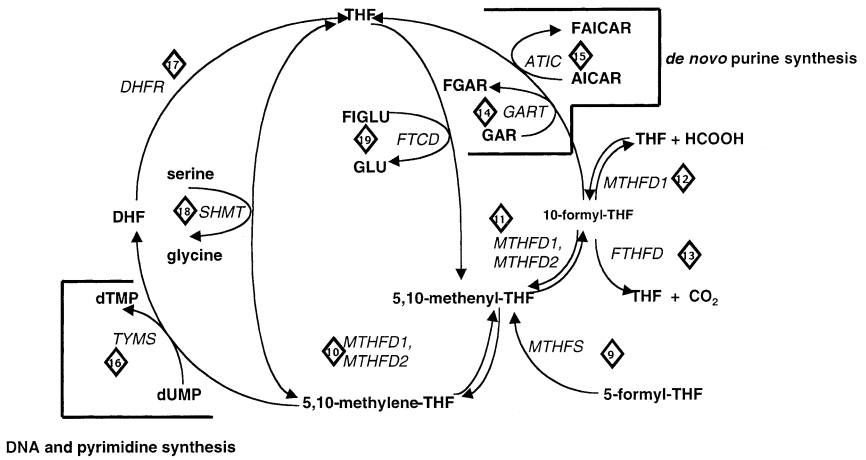

Fig. 2. Folate metabolism. Folate and homocysteine pathways are interrelated and are linked by 5,10-methylene-THF. Labels: 5,10-methenyl-THF synthase [MTHFS, step 9]; methylene-THF dehydrogenase, 5,10-methenyl-THF synthase, NAD-dependent [MTHFD2; a bifunctional enzyme; steps 10, 11]; 10-formyl-THF synthase and methenyl-THF cyclohydrolase [MTHFD1; a trifunctional enzyme; steps 10, 11, 12]; 10-formyl-THF dehydrogenase [FTHFD, step 13]; GAR (5-phosphoribosylglycineamide) transformylase [GART, step 14]; AICAR (5-phosphoribosyl-5-aminoimidazole-4-carboxamide) transformylase [ATIC, step 15]; thymidylate synthase [TYMS, step 16]; dihydrofolate reductase [DHFR, step 17]; serine hydroxymethyltransferase [SHMT, step 18]; glutamate fomiminotransferase and fomimino-THF cyclodeaminase [FTCD; a bifunctional enzyme, step 19].

notypes similar to birth defects and adult diseases associated with hyperhomocysteinemia in humans, such as neural tube defects and cancer. By testing whether HCY levels and expression profiles are altered in these single-gene mutant mice, we can begin to identify genes and processes that adversely affect homocysteine metabolism. This phenotypic-driven approach does not make assumptions about the identity of genes or biochemical processes that control HCY levels. As a result, we may discover novel and unexpected influences on HCY metabolism.

This study revealed mutant mice in which HCY levels were significantly elevated as a consequence of the mutation compared with their wild-type controls. We also found significant differences in gene expression patterns, often involving genes in the folate-homocysteine pathways in these mutant versus control comparisons. These differences provide clues to new genes, pathways, and functions that adversely affect folate-homocysteine metabolism.

Materials and methods

Mice. Mice were purchased from The Jackson Laboratory (Bar Harbor Maine), except for the *Ptch1* and *Ski* mutant and their wild-type controls. Mice were either bled upon their arrival or were maintained under SPF conditions. All mice shared the same animal room with controlled temperature, humidity, and 12-h light-dark cycle. Mice were provided food and water *ad libitum.* Number of animals used per mutants and controls: C57BL/6J, n = 30; C57BL/6J-*Pax3*^{Sp}, n = 14; C57BL/6J-*Apc*^{min}, n = 12; C57BL/6J-*Gli3*$^{Xt.J}$, n = 7; C57BL/6J-*Apob*^{tm1Unc}, n = 5; C3HeB/FeJLe, n = 4; C3HeB/FeJL*Gli3*^{Xt}, n = 10; *Ptch1*$^{+/+}$, n = 7; *Ptch1*$^{+/-}$, n = 5; *Ski*$^{+/+}$, n = 5; *Ski*$^{+/-}$, n = 5. Controls for *Ptch1*$^{+/-}$ and *Ski*$^{+/-}$ consisted of their wild-type sibs *Ptch1*$^{+/+}$ and *Ski*$^{+/+}$ respectively, from a segregating cross.

Diets. All mice were maintained on the Harlan-Teklad LM-485 diet, except for PTCH1 mice, which were maintained on the Prolab RMH 3000 diet.

Blood and tissue samples. Blood samples were obtained from the suborbital sinus of virgin female mice that were 6–8 weeks old and were collected in non-heparinized tubes. After centrifugation, serum samples were stored at −80°C. At autopsy, liver samples were placed immediately on dry ice.

Plasma versus serum test. Blood samples were obtained from the suborbital sinus of virgin (A/J × C57BL/6J)F_1 hybrid female mice that were 6–8 weeks old. Each sample was collected in non-heparinized tubes (serum) and heparinized tubes (plasma; potassium-EDTA microvette CB300 tubes, Sarstedt). After centrifugation, serum samples were stored at −80°C.

Homocysteine and methylmalonic acid measurements. Homocysteine and methylmalonic acid levels were measured with either GC/MS or HPLC methods.

MS/GC. Mouse serum samples (100 μl–200 μl) were diluted to 0.5 ml with PBS. Then 1 ml of dH_20 was added along with octadeuterohomo-

cysteine and trideutero-MMA internal standards (20 μl each of 165 and 25.8 μg/ml saline solutions, respectively). The samples were reduced by the addition of 51 μl dithiothreitol (10 mg/ml in 1 mol/L NaOH) and heated at 37°C for 30 min, and then applied onto a column of AG MP-1 resin (400 mg). The column was washed successively with 9 ml of dH_20, 3 ml of methanol, 1.2 ml of 0.3 mol/L acetic acid in methanol (to elute homocysteine), and finally, 1.2 ml of 3.6 mol/L acetic acid/0.1 mol/L HCl in 1:9 dH_2O:methanol (to elute MMA). The eluates were evaporated to dryness under vacuum. The homocysteine and MMA fractions were derivatized with 50 μl of BSTFA and 50 μl MTBSTFA, respectively (50°C for 30 min). The derivatization mixtures were then mixed in autoinjector vials and analyzed with an HP5988 in positive ion El mode. Chromatography was on a 30 m × 0.25 mm capillary column coated with a 0.25 μm DB-1 film. Injection was in splitless mode with a 1-min delay at 100°C and then ramped to 180°C at 40°C/min, then to 210°C at 5°C/min, followed by a 3-min bake-out at 280°C. Under these conditions, MMA-2TBDMS and homocysteine-3TMS elute in that order 7 min after injection and about 8 s apart. Ions monitored were m/z 289 (Do-MMA-2TBDMS), 292 (D3-MMA-2TBDMS), 234 (Do-homocysteine-3TMS), and 238 (D4-homocysteine-3TMS

HPLC. The HPLC method of Ubbink and Vermaak (1991) was used to measure total serum homocysteine levels.

Reagents for the array. Gene and EST databases were surveyed to identify sequences for genes involved in folate-homocysteine metabolism or in other pathways as controls. The sequence of each candidate PCR product was evaluated for motifs, repeats, and closely related gene family members that might confound its specificity in expression profile experiments. Eight genes (AHCY, AMS, DHFR, LEPR, NRAMP, PLI, RFC, and TYMS) were represented by two PCR products, one for the 5′ end of the gene and the other for the 3′ end of the gene. Oligonucleotides were synthesized by Research Genetics (Huntsville, Ala.).

PCR products for expression arrays. Trizol Reagent kits (Gibco BRL) were used to prepare total RNA from fresh or frozen tissues (usually liver) from female C57BL/6J mice. cDNAs made from these RNAs (Superscript II RNase H-Reverse Transcriptase; Gibco BRL) were used as template in PCR reactions. The resulting PCR products were purified and quantitated. To make the arrays, 160 ng of purified and denatured PCR products were aliquoted in duplicate on Hybond N+ nylon membranes (Amersham).

Hybridization probes. To make the hybridization probe, 20 μg of total RNA was radiolabeled with ^{32}P-deoxycytosine (dCTP) in first-strand cDNA synthesis reactions (Superscript II RNase H-Reverse Transcriptase; Gibco BRL). Hybridizations were done at 65°C for 20–24 h in Church buffer after pre-hybridization at 65°C for 2–3 h. Four replicate pools from each strain or mutant were prepared by combining equal portions (by weight) of liver samples from the same four to five genetically and phenotypically identical mice. The radiolabeled cDNA pools were independently hybridized to new replicate membrane arrays. A phosphorimager (Molecular Dynamics) was used to quantitate hybridization signals.

Data analysis. Each gene was represented twice on each array to control for the variation in background noise on the nylon membrane. A correlation coefficient for the duplicate spots was calculated. If the correlation coefficient fell below 0.99, inconsistent duplicate data points were discarded. The expression values were log transformed and normalized by center mean, similar to the procedure used in the Cluster program (Eisen et al. 1998) to account for the variation in probe intensity between replicate membranes. The normalized values for the four replicate membranes were used to calculate the mean and the standard deviation. If the signal for a gene in one of the four replicates exceeded 2 standard deviations from the mean, the remaining three data points were used for the analysis. For the majority of genes, the estimate of the expression level for each gene was based on eight signals.

In more detail, the null hypothesis is that $X_{ijk} = M_i G_j R_k (1 + E_{ijk})$, where X_{ijk}, M_i, G_j, and R_k are the expression level, strain or mutant effect, gene effect and replicate effect, respectively, such that the replicates are indexed separately by k within each strain. E_{ijk} is an error term that is identically and independently distributed for each reading. Taking the natural logarithm of both sides, we obtain $y_{ijk} = m_i + g_j + r_k + e_{ijk}$, where y_{ijk}, m_i, g_j, and r_k are the log of X_{ijk}, M_i, G_j and R_k, respectively, and $e_{ijk} \sim E_{ijk}$ are independently and identically distributed normal errors. To accurately estimate the gene effects, we set $r_k \sim \delta_j x_{ijk} / n$, where n is the number of genes in the replicate, and letting $y_{ijk} = x_{ijk} - r_k$, we used the model $x_{ijk} = m_i + g_j + e_{ijk}$, where k now indexes the several identically distributed measures for each combination of strain and gene. For each cell C_{ij} we can calculate the mean y_{ij} and the standard deviation s. Those s that exceeded the critical value $s^* = 1.96$ were considered to result from at least one aberrant measure. Where possible, these values are removed, and the entire analysis is repeated on the edited data. For the 2520 signals in the $120 = (15 \times 16)/2$ pairwise comparisons, only 4.1% had to be eliminated.

We next examined the RNA abundance data to identify outliers in each pairwise mutant versus control comparisons. To do this, the control normalized values were subtracted from the mutant normalized values across all the genes. Then, genes falling outside of the 95% confidence interval were considered outliers.

We inspected the cell means y_{1jk} and y_{2jk} for each gene j and noted those where the variation exceeds $\delta = 1.96$, as indicating significantly heterogeneous levels of gene expression in the two strains. Although we formally included strain effects in our model, we were really interested only in the interactions of gene and strain, and any main effect due to strain was removed along with the replicate effect in defining y_{ijk}, because of the nesting structure of the experimental design. The critical values s* and δ are determined from the mean squared error remaining after all gene effects and (negligible) strain effects have been removed.

Northern analysis. Gene expression levels were validated for TYMS 3′ and 5′ end in B6 and B6-*Pax3^{Sp};* FBP2 in B6, B6-*Pax3^{Sp}, Ski$^{+/+}$* and *Ski$^{+/-}$*; AHCY 3′ and 5′ end in B6 and B6-*Gli3$^{Xt.J}$*. Beta actin and glyceraldehyde-3-dehydrogenase were used as controls to normalize differences in mRNA loading. Total RNA from liver was extracted using a Trizol Reagent kit (Gibco BRL), and messenger RNA was isolated with the Oligotex mRNA Midi Kit (Qiagen). The mRNA was transferred onto Hybond N+ nylon membranes (Amersham), and the hybridization was performed with the NorthernMax kit (Ambion). Probes were radiolabeled with ^{32}P-deoxycytosine (dCTP) by PCR. A phosphorimager (445SI, Molecular Dynamics) was used to quantitate hybridization signals.

Results

Serum homocysteine levels in mutant mice. Serum homocysteine levels were measured in mutant mice with single-gene mutations (Fig. 3A and 3B). The criteria for selecting mutant mice for this study was their propensity to cause disorders, such as neural tube defects and cancer, that are similar to anomalies associated with hyperhomocysteinemia in humans (Mudd et al. 2001; Rosenblatt and Fenton 2001). Female mice were used because in humans maternal hyperhomocysteinemia is a risk factor for fetal neural tube defects (Malinow et al. 1998), although anomalies in fetal metabolism also appear to be important (Fleming and Copp 1998). Virgin female mice were used to control for possible effects of pregnancy on HCY levels (Kang et al. 1986; Steegers-Theunissen et al. 1997). Levels were measured in heterozygous *Apob^{tmlUnc}, Pax3^{Sp}, Apc^{min}, Ptch1$^{+/-}$*, *Ski$^{+/-}$*, and *Gli3$^{Xt.J}$* compared with their respective wild-type (+/+) controls (Fig. 3). Because homozygotes for these mutations show anencephaly or spina bifida and die during embryogenesis (Mouse Locus Catalog; www.informatics.jax.org), it was not possible to collect sufficient blood from these fetuses to measure HCY levels.

Because protein content can vary between plasma and serum, and because homocysteine is mainly protein bound, levels were compared in serum and plasma. Plasma and serum samples were obtained by collecting blood from the retro-orbital sinus of virgin female $(A/J \times C57BL/6J)F_1$ hybrids that were 6–8 weeks old. Homocysteine levels were not significantly different between plasma and serum (mean HCY level in serum: 5.5 ± 1.1 μmol/L; mean HCY in plasma: 4.9 ± 0.7 μmol/L; paired two-tailed Student's t test, $p = 0.18$). HCY levels were, therefore, measured in serum samples in the following studies.

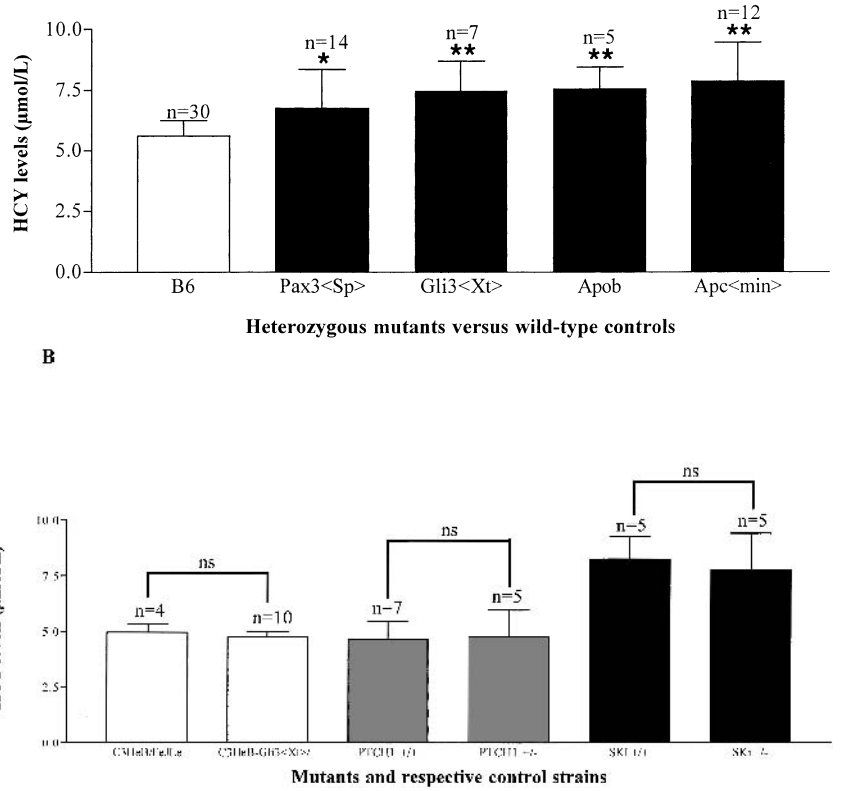

Fig. 3. Homocysteine levels for mutant mice and their respective wild-type controls. **A.** Homocysteine levels for mutants congenic on the B6 background. Mean homocysteine levels (μmol/L) for: B6, 5.6 ± 0.6; *Pax3*^{Sp}, 6.8 ± 1.6; *Apc*^{min}, 7.8 ± 1.6; *Gli3*^{XtJ}, 7.4 ± 1.2; *Apob*^{tmlUnc}, 7.5 ± 0.9. To assess differences in mean HCY levels, Dunnett's test was used. Values are expressed as mean ± standard deviation. *P < 0.05, **P < 0.01. **B.** Homocysteine levels for mutants on different backgrounds. Mean homocysteine levels (μmol/L) for: C3HeB/FeJLe, 5.0 ± 0.4; C3HeB/FeJLe-*Xt*, 4.7 ± 0.3; *Ptch1*$^{+/+}$, 4.6 ± 0.8 and *Ptch1*$^{+/-}$, 4.7 ± 1.2; *Ski*$^{+/+}$, 8.3 ± 1.0 and *Ski*$^{+/-}$, 7.7 ± 1.6. Controls for *Ptch1*$^{+/-}$ and *Ski*$^{+/-}$ consisted of their wild-type sibs from a segregating cross. To assess differences in mean homocysteine levels, Student's t test was used. Values are expressed as mean ± standard deviation; ns, non significant.

When compared with their respective controls, *Apc*^{min}, *Apob*^{tmlUnc}, *Gli3*^{XtJ}, and *Pax3*^{Sp} mice had significantly higher HCY levels than the C57BL/6J (B6) background control strain (Fig. 3A). The average level increased by 18% in *Pax3*^{Sp}, 24% in *Gli3*^{XtJ}, 25% in *Apob*^{tmlUnc}, and 31% in *Apc*^{min} mice. *Gli3*^{XtJ} (on the C3HeB/FeJ background), *Ptchl*$^{+/-}$, and *Ski*$^{+/-}$ showed substantial overlap with their respective *Ptchl*$^{+/+}$ and *Ski*$^{+/+}$ wild-type control (Fig. 3B). These results show that several single-gene mutations adversely affect folate and HCY metabolism and that the effect can depend on genetic background. *Pax3* and *Gli3* are part of the hedgehog signal transduction pathway (Dominguez et al. 1996; Goodrich et al. 1996; Gorlin 1987), *Apc* contributes to WNT signal transduction (Behrens et al. 1998), and *Apob* participates in lipid metabolism (Farese and Herz 1998). This is the first evidence that mutations in these pathways adversely affect folate-homocysteine metabolism.

To test whether vitamin B_{12} (cobalamin) deficiency might be responsible for elevated HCY levels, methylmalonic acid (MMA) levels were measured (Gilfix et al. 1997; Ubbink et al. 1991) in selected inbred strains and mutant mice. Vitamin B_{12} deficiency is associated with increased MMA levels (Stabler et al. 1986). Methylmalonyl-CoA mutase requires vitamin B_{12} as a cofactor, whereas methionine synthase (MTR) requires both folic acid and vitamin B_{12} as cofactors (Kirke et al. 1993). If vitamin B_{12} was deficient, both MMA and HCY levels should be elevated. However, none of the mice with elevated HCY had high MMA levels (data not shown), arguing that these cases of homocysteinemia did not result from vitamin B_{12} deficiency.

Expression studies on mutant mice. Expression profiles (Brown and Botstein 1999; Duggan et al. 1999; Tamayo et al. 1999) are a powerful method to identify genes whose RNA abundance is modulated in mutant mice. Arrays of gene-specific PCR products (Bertucci et al. 1999; Gress et al. 1992) were used to compare profiles as a way of testing whether the RNA abundance of genes in folate-homocysteine metabolism was altered in mutant versus control mice. These arrays were composed of most (25 out of 27) of the genes involved in folate-homocysteine metabolism (46.7%), with the remaining 28 genes (53.3%) being functionally unrelated to this pathway (Table 1; MTHFS, step #9 of Fig. 2, and FTHFD, step #13 of Fig. 2, were not included because sequences were not available when these experiments were conducted). Liver was used as a source of RNA because folate-homocysteine metabolism occurs primarily in this organ (Mudd et al. 2001; Rosenblatt and Fenton 2001). Arrays were hybridized with four replicate pools of radiolabeled total liver cDNA from the same mutants and controls that were used for the homocysteine survey. Raw data are available on the following website: "http://genomics.cwru.edu/download.html".

Two methods were used to identify outliers in each mutant versus wild-type control comparison: 1) two standard deviations from the mean expression level for all genes, and 2) greater than three-fold difference in RNA level (see Materials and Methods for a detailed description of the data analysis). Because only heterozygotes could be tested, any changes in RNA abundance were expected to be subtle. Interestingly, the observed changes ranged between two- and eight-fold. Twelve genes, eight of which were directly involved in folate-homocysteine metabolism, showed a difference of at least 2 standard deviations, and two additional genes differed at least three-fold in expression levels (Table 2). For instance, FBP2 levels were significantly increased 4.9-fold, and GNMT levels were decreased 3-fold in heterozygous B6-*Pax3*^{Sp} mutants compared with B6 wild-type controls. In general, the increases ranged from 1.8-fold for AHCY in C3HeB- *Gli3*^{XtJ} to

Table 1. List of genes used on the arrays. The name and symbol of the genes, as well as to which pathway the genes belong, are indicated. The DNA sequences (Genbank accession number) and the portion of the genes (bases) used for the design of PCR products are also indicated. Eight genes (AHCY, AMS, DHFR, LEPR, NRAMP, PLI, RFC and TYMS) were represented by two PCR products, one for the 5′ end of the gene and the other for the 3′ end of the gene.

Genes Name	Symbol	Genbank acc#	Bases	Pathway
Adenosylhomocysteine hydrolase 3′ end	AHCY 3′	L32836	1369–1874	Hcy-Folate
Adenosylhomocysteine hydrolase 5′ end	AHCY 5′	L32836	171–619	Hcy-Folate
Plasmin inhibitor alpha 2 3′ end	PLI 3′	Z36774	951–1458	Inflammatory response
Plasmin inhibitor alpha 2 5′ end	PLI 5′	Z36774	207–626	Inflammatory response
Apolipoprotein E	APOE	M12414	352–843	Cholesterol synthesis and transport
Beta actin	ACTB	X03672	294–893	WNT signal transduction
Betaine homocysteine methyltransferase	BHMT	W16199	89–315	Hcy-Folate
Breast Cancer 1	BRCA1	U36475	5997–6398	Unknown
Cart1 Cartilage homeoprotein 1	CART1	X92346	1052–1455	Unknown
Cystathionine beta-synthase	CBS	AA096720	25–236	Hcy-Folate
C reactive protein	CRP	X17496	222–679	Inflammatory response
Ceruloplasmin	CP	U49430	2278–2714	Inflammatory response
UDP galactose ceramide-galactosyl transferase	CGT	X92122	441–850	Inflammatory response
Cystathionine gamma lyase	CTH	W11479	114–316	Hcy-Folate
Dihydrofolate reductase 3′ end	DHFR 3′	L26316	795–1253	Hcy-Folate
Dihydrofolate reductase 5′ end	DHFR 5′	L26316	62–478	Hcy-Folate
5-Phosphribosyl-5-aminoimidazole-4-carboxamide transformylase	ATIC	W08334	116–318	Hcy-Folate
Folate binding protein 1	FOLBP1	M64782	260–699	Hcy-Folate
Folate binding protein 2	FOLBP2	M64817	402–896	Hcy-Folate
Fibrinogen A alpha polypeptide	FGA	D43759	72–571	Inflammatory response
Glyceraldehyde-3-phosphate dehydrogenase	GAPD	M32599	322–910	Glycolysis
Glutamate formininotransferase	FTCD	A5A01787	175–466	Hcy-Folate
Gli3	GLI3	X95255	317–884	Hedegehog signal transduction
Glucose transporter 1	GLUT	D10230	26–544	Glucose transport
Glycine N-methyltransferase	GNMT	W83078	202–420	Hcy-Folate
Haptoglobin	HP	M96827	165–672	Inflammatory response
Heme oxygenase 1	HMOX1	X13356	181–587	Inflammatory response
Inositol triphosphate type 2 receptor	ITPR2	Z71173	2436–7837	Inositol signal transduction
Inositol triphosphate type 3 receptor	ITPR3 3	Z71174	169–571	Inositol signal transduction
Inositol polyphosphate-1 phosphatase	INPP1	U27395	912–1314	Inositol signal transduction
Inositol polyphosphate-5 phosphatase	IPOLY5	W17555	130–358	Inositol signal transduction
Leptin receptor 3′ end	LEPR 3′	U43667	3779–4352	Unknown
Leptin receptor 5′ end	LEPR 5′	U42467	24–516	Unknown
Methenyl cyclohydrolase, mitochondrial	MTCH	D21754	139–357	Hcy-Folate
5-Methyltetrahydrofolate-homocysteine methyltransferase (methionine synthase)	MTR	Shane B, pers. communication		Hcy-Folate
5, 10-Methylenetetrahydrofolate reductase	MTHFR	AA183742	114–359	Hcy-Folate
Neuropeptide Y receptor Y1	NPY1R	Z1438069	851–1363	Unknown
Neuropeptide Y receptor Y6	NPY6R	U58367	1518–1918	Unknown
Natural resistance-associated macrophage protein 1	NRAMP1	L13732	1014–1422	Inflammatory response
Natural resistance-associated macrophage protein 2 3′ end	NRAMP2 3′	L33415	1083–1492	Inflammatory response
Natural resistance-associated macrophage protein 2 5′ end	NRAMP2 5′	L33415	167–588	Inflammatory response
Oncostatin M	OSM	D31942	339–800	Inflammatory response
Plasminogen activator inhibitor type 1	PAI1	M33960	180–741	Inflammatory response
Transthryretin (Prealbumin)	TTR	X03351	57–376	Inflammatory response
5-Phosphoribosylglycineamide transformylase	GART	U01024	2481–2896	Hcy-Folate
Reduced folate carrier 3′ end	RFC 3′	U32469	1663–2233	Hcy-Folate
Reduced folate carrier 5′ end	RFC 5′	U32469	314–731	Hcy-Folate
Serum amyloid A5	SAA5	U02554	162–509	Inflammatory response
S-adenosylmethionine synthetase 3′ end	AMS 3′	L.13622	2575–3058	Hcy-Folate
S-adenosylmethionine synthetase 5′ end	AMS 5′	L.13622	302–706	Hcy-Folate
Serum amyloid P-component	SAP	X14079	195–634	Inflammatory response
Serine hydroxymethyltransferase, cytoplasmic	SHMT1	AA028497	250–477	Hcy-Folate
NADP+ dependent methylenetetrahydrofolate dehydrogenase cyclohydrolase synthetase	MTHFD	J04627	1377–1907	Hcy-Folate
Thymidylate synthase 3′ end	TYMS 3′	M13019	432–863	Hcy-Folate
Thymidylate synthase 5′ end	TYMS 5′	M13019	32–458	Hcy-Folate

5.6-fold for ATIC in B6- *Apc*^{min} mice. The decreases ranged from 1.8-fold for SHMT in B6- *Apob*^{tmlUnc} to 7.9-fold for TYMS in B6-*Pax3*^{Sp}. Therefore, 36% of HCY-folate genes used in the array (9/25) have altered expression levels.

Results for GLI3 are noteworthy in two respects. First, the increase in GLI3 RNA abundance in mice that were partially deficient for PTCH1 (Table 2) and its decrease in mice partially deficient for PAX3 are consistent with the inhibitory effect of PTCH1 on GLI3 function (Murone et al. 1999) and the activating influences of GLI3 on PAX3 function (Dahl et al. 1997). Second, the GLI3 RNA level decreased in both B6-*Pax3* and *Apc* mutant mice, both of which showed elevated HCY levels compared with their controls, whereas the GLI3 levels increased in *Ptch* mutant mice, which showed HCY levels similar to their control. The association between changes in HCY levels and GLI3 RNA levels suggests that a correlation, and perhaps a causal relation, might be involved.

Results for TYMS in *Pax3*^{Sp} mutant mice are also noteworthy. These mutant mice are thymidine deficient (Fleming and Copp 1998), and this may result from TYMS down-regulation (Table 2; thymidine is represented as dTMP in Fig. 2). Therefore, these results are consistent with known physiological processes.

The outlier genes AHCY, LEPR, RFC, and TYMS were each represented by two PCR products, one for the 5′ end and the other for the 3′ end of the gene. There was no correlation in expression level between the 5′ and 3′ probes for each of these genes; i.e., only one of the products was altered in the mutant versus control comparison: TYMS 3′, AHCY 5′, RFC 3′, and LEPR 5′ in B6-*Pax3*^{Sp} mice; LEPR 3′ in *Apc*^{min}; AHCY 5′ in C3HeB-*Gli3*^{XtJ}; and RFC 3′ in *Ski* mice. These results raise the possibility that

Table 2. Significant differences (≥ 2 standard deviation) in RNA abundance in mutants compared with their respective wild-type controls. The effect on HCY levels and the type of neural tube defect phenotype are listed. RNAs that are directly involved in folate-homocysteine metabolism (Figs. 1 and 2) are shown in **bold.** The genes that were below the two-standard-deviation threshold but showed changes equal or higher than 3-fold were also evaluated and are *underlined.* For instance, HCY levels are increased and SHMT expression levels are decreased in heterozygous C57BL/6J-*Apob*^{tm1Unc} compared with the B6 wild-type control. Abbreviations: SHMT, serine hydroxymethyltransferase; INPP1, inositol polyphosphate-1 phosphatase; FBP2, folate-binding protein-2; GNMT, glycine N-methyltransferase; GLI3, transcription factor Gli3; LEPR, leptin receptor; SAP, serum amyloid P-component; TYMS, thymidylate synthase; ATIC, 5-phosphoribosyl-5-aminoimidazole-4-carboxamide transformylase; AHCY, adenosylhomocysteine hydrolase; MTHFR, 5,10-methylenetetrahydrofolate reductase; GART, 5-phosphoribosylglycineamide transformylase; SAA5, serum amyloid A5; RFC, reduced folate carrier; SAP, serum amyloid P.

Heterozygous Mutants	Control	Effect on HCY Levels	Neural Tube Defect	RNA Abundance	
				Increased	Decreased
B6-Apob	B6	Increased	Exencephaly[a]		SHMT, 1.8X
B6-Pax3⟨Sp⟩	B6	Increased	Exencephaly and spina bifida[a]	**FBP2, 4.9X** **ATIC, 3.4X** INPP1, 3.2X	TYMS, 7.9X SAP, 4.9X **GNMT, 3.0X** LEPR, 3.7X GLI3, 3.4X
B6-Apc⟨min⟩	B6	Increased	No obvious defect[b]	**ATIC, 5.6X** LEPR, 3.4X	GLI3, 3.8X
B6-Gli3⟨Xt⟩	B6	Increased	Exencephaly[c]		**AHCY, 3.5X**
C3HeB-Gli3⟨Xt⟩	C3HeB/FeJLe	Unchanged	Exencephaly[c]	**AHCY, 1.83X** **MTHFR, 2X**	
Ptch1	Ptch1 +/+	Unchanged	Spina bifida[d]	**GART, 2.5X** GLI3, 2.4X SAA5, 2.5X	
Ski	Ski +/+	Unchanged	Exencephaly[a]	**FBP2, 3.0X**	RFC, 2.0X

[a] Harris and Juriloff 1999.
[b] C57BL/6J-*Apc*^{Min} mice show colon cancer, but no obvious neural-tube defect.
[c] Green 1989
[d] Goodrich et al. 1997; these mice also show a medulloblastoma phenotype.

these genes are alternatively spliced. Review of the literature reveals evidence that both LEPR (Mercer et al. 1996) and RFC (Tolner et al. 1997) produce alternative transcripts. Our LEPR 3′ PCR product detected the ob-r transcript, whereas the LEPR 5′ PCR product detected the a, b, d and e transcripts. Moreover, Mercer and coworkers also found expression differences between LEPR 3′ and 5′ sequences in various mouse brain regions (Mercer et al. 1996). By contrast, our 5′ and 3′ PCR products did not distinguish the alternative RFC transcripts. To test whether the other two genes, AHCY and TYMS, produce alternative transcripts, we performed a Northern analysis of liver mRNA from B6 and B6-*Pax3*^{Sp} for TYMS, and from B6 and B6-*Gli3*^{XtJ} for AHCY. Expression differences between the 5′ and 3′ end sequences were confirmed for AHCY but not for TYMS (data not shown). Finally, the sequence of the human genome reveals an average of 3–4 alternative transcripts per gene (International Genome Sequencing Consortium, 2001; Venter et al. 2001), and it is likely that many genes in mice also have alternative transcripts.

Because of the inherent nature of the data analysis for expression profiles, some outlier genes are expected to be 'false positives', at least with respect to their association with changes in HCY levels. Two examples are suggested in this survey. FBP2 levels increased in both *Apob* and *Ski* mutant mice (Table 2). *Apob* mutant mice showed elevated HCY levels, whereas *Ski* mutant mice showed unchanged HCY levels. Similarly, LEPR levels decreased in B6-*Pax3* mutant mice and increased in B6-*Apc* mutant mice. Both *Apob* and *Ski* mutants showed elevated HCY levels compared with their controls. Thus, for both FBP2 and LEPR, there does not seem to be a simple relationship between changes in HCY and RNA levels. Whether results for FBP2 and LEPR are 'false positives' or instead reflect more complex relations between HCY levels and RNA abundance remains to be determined.

Validation studies. Gene expression levels in liver samples were independently measured with Northern analysis for TYMS (probes for the 5′ and 3′ portion of the gene) in B6 and B6-*Pax3*^{Sp}; FBP2 in B6, B6-*Pax3*^{Sp}, and in *Ski*$^{+/+}$ and *Ski*$^{+/-}$; AHCY 5′ (the 3′ end is not detected on the array and, therefore, could not be included in the validation) in B6 and B6-*Gli3*^{XtJ}. These results were compared with those for the corresponding genes on the array between the mutants and their respective controls. With beta actin and GAPDH as controls for normalization, the correlation between expression levels for the Northerns and arrays was 0.95 (actin control: $N = 5$, $P < 0.05$) and 0.89 (GAPDH control: $N = 5$, $P < 0.05$). Thus, expression levels for Northerns and arrays were highly concordant in all 10 comparisons.

Discussion

Given the complex relationships between the folate and homocysteine pathways on various birth defects and adult diseases, we studied HCY levels in mutant mice with phenotypes (NTDs and colon cancer) often associated with hyperhomocysteinemia in humans. Mice with mutations in the *Apob, Gli3, Pax3, Ptch,* and *Ski* genes were used as models for NTDs, and mice with a mutation in the *Apc* gene as a model for colon cancer. Serum homocysteine levels were measured and hepatic gene expression profiles were monitored in heterozygous mutants, because homozygotes are embryonic lethal. An important attribute of surveying heterozygous mutants is the ability to test for subtle and specific consequences of partial protein deficiencies as compared with the severe phenotypic and metabolic abnormalities that occur in homozygous mutants. Partial deficiencies of APC, APOB, PAX3, and GLI3 (on the B6 background) increased HCY levels, whereas PTCH, SKI, and GLI3 (on the C3H background) did not affect HCY levels. We also found significant differences in gene expression patterns, often affecting folate-homocysteine metabolism, in these mutants. These results provide clues to new pathways, i.e., WNT and hedgehog signal transduction (APC, GLI3, and PAX3) and lipid transport (APOB) that adversely affect HCY metabolism and perhaps contribute to the pathogenesis of birth defects and adult diseases in these mice.

HCY levels in humans and mice. The magnitude of changes in HCY levels in mutant mice is comparable to that found in humans who are heterozygous for certain genetic mutations. In humans, for example, plasma HCY levels are elevated 50%–75% in heterozygotes for mutations in the CBS gene (Welch and Loscalzo 1998), whereas heterozygotes for the Ala / Val (C677T) mutation in the

Table 3. Summary of RNA abundance results showing consistent changes in gene expression levels unique to either mutant mice with elevated or mutant mice with unchanged HCY levels. Genes in bold are directly involved in the homocysteine-folate pathway. Expression of folate-homocysteine genes is often reduced in strains with elevated HCY levels (*Apob*^{tmlUnc}, *Pax3*^{Sp}, *Apc*^{min}, and B6-*Gli3*^{XtJ}), whereas their expression is often elevated in strains with normal HCY levels (C3HeB/FeJ-*Gli3*^{XtJ}, *Ptch1,* and *Ski*).

Mutants with Elevated HCY Levels		Mutants with Unchanged HCY Levels	
Genes Whose Expression Is Increased	Genes Whose Expression Is Decreased	Genes Whose Expression Is Increased	Genes Whose Expression Is Decreased
ATIC	**SHMT**	**MTHFR**	**RFC**
INPP1	**TYMS**	**AHCY**	
	GNMT	**GART**	
	AHCY	GLI3	
	GLI3	SAA5	
	SAP		

MTHFR gene have similar HCY levels as Ala/Ala (C/C) 'wild-type' homozygotes (Brattstrom et al. 1998). Gene targeting was used to create mice with targeted deficiencies of the CBS (Watanabe et al. 1995), MTR (Swanson et al. 2001), and MTHFR (Chen et al. 2001) proteins. Compared with their respective wild-type controls, heterozygous CBS mutant mice show a 50% increase in the HCY level (Watanabe et al. 1995), heterozygous MTR mutant mice show a 49% increase in HCY level in males and a 70% increase in females (Swanson et al. 2001), and heterozygous MTHFR mutant mice a 38% increase (Chen et al. 2001). In our survey, mutant mice that are prone to NTDs or colon cancer have HCY levels increased between 18% and 31% when compared with their wild-type control (Fig. 3). The differences between these results is that CBS, MTR, and MTHFR in humans and mice are directly involved in folate-homocysteine metabolism, whereas the mutant genes included in our survey are involved primarily in other developmental and physiological pathways, and their metabolic effects may be modulated as their effects are transmitted through various pathways. Differences in diet may also contribute to the modest differences between HCY levels in humans and mice. Dietary folate levels vary considerably in humans, whereas the mutant and control mice were maintained on defined diets. In the present study, mice were maintained on a relatively high folate diet (7.5 mg/kg). Nevertheless, the effects on HCY levels in these mutant mice are in the same direction and roughly of the same magnitude as those found in humans.

HCY metabolism and neural tube defects. Pregnant women with elevated HCY levels have an increased risk of giving birth to a child with a NTD (Mills et al. 1995). When taken before and during pregnancy, folic acid prevents most (70%) NTDs (MRC Vitamin Study Research Group 1991), demonstrating the critical role that folate-homocysteine metabolism plays in neural tube development.

Distinct sites of NTDs in mutant mice reflect regional differences in mechanisms of normal neural fold elevation and closure (Harris and Juriloff 1999). For instance, exencephaly is a failure of elevation of the neural folds in the region between the caudal border of the forebrain and rostral border of the hindbrain, whereas spina bifida is a failure to close the posterior neuropore (Harris and Juriloff 1999). Surveyed mice with exencephaly have both normal (C3HeB-*Gli3*^{XtJ} and *Ski*) and increased HCY levels (B6-*Apob*^{tmlUnc} and B6-*Gli3*^{XtJ}). B6-*Pax3*^{Sp} mice, which have both exencephaly and spina bifida, showed the smallest increase in HCY level (Table 2). Thus, a relation between the type or severity of neural tube defect and HCY levels in these mutant mice was not evident; a pattern might become apparent with a larger survey of mutants.

Folate-HCY metabolism and cancer. Mutations in the APC gene, a key component of the WNT transduction pathway, contribute to colorectal cancer in humans (Cottrell et al. 1992) and mice (Su et al. 1992), possibly by inducing chromosome instability (Fodde et al. 2001; Kaplan et al. 2001). The folate-homocysteine pathway is involved in important methylation reactions, DNA synthesis and repair, and chromosome stability (Fenech 2001). Disruption of folate and homocysteine pathways, for instance with low vitamin B12, methionine, and folate intake, is an important risk factor for many cancers (Fenech 2001). Moreover, dietary folate supplementation suppresses colonic polyps in B6-*Apc*^{min} mice in an age-dependent manner (Song et al. 2000). Finally, folate is used as a therapeutic against colon cancer (Janne and Mayer 2000). The elevated HCY level (Fig. 3A), as well as the changes in RNA abundance levels (Table 2) in *Apc* mutant mice, provide a new model for studying the relations between WNT signal transduction, folate-homocysteine metabolism, and susceptibility to colon cancer.

HCY levels and expression profiles. HCY levels and expression profiles were monitored in heterozygous B6-*Apc*^{min}, B6-*Apob*^{tmlUnc}, B6-*Gli3*^{XtJ}, B6-*Pax3*^{Sp}, *Ptch1*$^{+/-}$, *Ski*$^{+/-}$ and C3HeB-*Gli3*^{XtJ} mutant mice to study the physiological and molecular responses of folate-homocysteine metabolism to specific genetic perturbations. The biochemical functions of the outlier genes in the mutant versus control comparisons were evaluated to gain clues to the basis for elevated versus unchanged HCY levels in mice with partial deficiencies of APOB, PAX3, APC, GLI3, PTCH1, and SKI proteins (Table 2). If these mutations adversely affect folate-homocysteine metabolism, the changes in RNA abundance levels should be consistent with particular physiological consequences, assuming that changes in RNA abundance result in altered functional activities.

One of several provocative differences among the mutant mice is that expression of folate-homocysteine genes is often reduced in strains with elevated HCY levels (*Apob*^{tmlUnc}, *Pax3*^{Sp}, *Apc*^{min} and B6-*Gli3*^{XtJ}), whereas their expression is often elevated in strains with normal HCY levels (C3HeB/FeJ-*Gli3*^{XtJ}, *Ptch1,* and *Ski*) (Table 3). Perhaps C3HeB/FeJ-*Gli3*^{XtJ}, *Ptch1,* and *Ski* mice are able to maintain normal levels by increasing the levels of transcription of these genes, despite their sensitizing mutation (Table 2).

The decreased GNMT transcript levels in *Pax3*^{Sp} mice are associated with increased HCY levels, perhaps because of glycine hypomethylation (Table 2). GNMT (glycine N-methyltransferase) transfers the methyl group of *S*-adenosylmethionine to glycine (Ogawa et al. 1998). A population study showed that DNA hypomethylation is associated with elevated HCY levels (Yi et al. 2000). Whether deficiency of other methyltransferases results in elevated HCY levels in *Pax3*^{Sp} mice, as well as the relation between PAX3 and GNMT, remains to be determined.

Genetic background may account for the contrasting effects on AHCY and HCY levels. Under normal physiological conditions, the condensation of adenosine and HCY to form S-adenosylhomocysteine is favored, a reaction that decreases HCY levels (Fig. 1,

reaction #6; Finkelstein 1990). Therefore, the reduced level of AHCY in *Gli3*$^{Xt.J}$ mutant mice on the C57BL/6J background may account for their increased HCY (Table 2). By contrast, the *Gli3*$^{Xt.J}$ mutation on the C3HeB/FeJ background shows increased AHCY levels and normal HCY (Table 2). The nature of this genetic background effect remains to be determined.

An inverse relationship between folate and HCY levels is often found (Rosenblatt and Fenton 2001). Increasing the availability of folate, which might result from increased in ATIC, FBP2, MTHFR, and GART observed in *Pax3*^{Sp}, *Apc*^{min}, C3HeB/FeJ-*Gli3*$^{Xt.J}$; *Ptch1,* and *Ski* mice, should reduce HCY levels. However, *Pax3*^{Sp} and *Apc*^{min} mice seem incapable of adequately regulating their HCY levels by this mechanism. Consistent with this interpretation is the observation that prenatal treatment with folate corrects NTD in *Pax3*^{Sp} mice (Fleming and Copp 1998), suggesting that these mice are folate deficient.

Summary. Our phenotype-based approach, based on measurement of HCY levels and expression profiles in mice with single-gene mutations, has provided clues to the identity of novel genes and pathways that adversely affect folate and homocysteine metabolism. Although the relations between reactions in folate-homocysteine metabolism are complex (Kisliuk 1999), making it difficult to predict the metabolic consequences of many perturbations, the consistency between elevated HCY levels, altered RNA abundance levels, and metabolic expectations is provocative. The changes in gene expression are consistent with the literature, but will have to be assessed in more detail by measuring additional biological markers, such as purine and thymidine levels and global methylation.

We thank Robert E. MacKenzie and Shawn McCandless for many valuable discussions about the biochemistry of folate and homocysteine metabolism, and Barry Shane for the methionine synthase sequence prior to publication. This work was supported by grants from the March of Dimes Foundation and from the National Heart, Lung and Blood Institute (HL58982) to J.H.Nadeau, the National Institute of Child Health and Development (HD30728) to C. Colmenares, the Medical Research Council to D.S. Rosenblatt, the Natural Science and Engineering Research Council of Canada and the Canadian Genome Analysis and Technology Program to D.Sankoff, by a grant from the Charles B. Wang Foundation to the Center for Computational Genomics, by a grant from the Keck Foundation to the Department of Genetics, and by a Howard Hughes Medical Institute grant to Case Western Reserve University School of Medicine. B. Christensen was a recipient of a fellowship from the Royal Victoria Hospital Research Institute. D. Sankoff is a fellow of the Canadian Institute for Advanced Research.

References

Behrens J, Jerchow BA, Wurtele M, Grimm J, Asbrand C et al. (1998) Functional interaction of an axin homolog, conductin, with beta-catenin, APC, and GSK3beta. Science 280, 596–599

Bertucci F, Bernard K, Loriod B, Chang YC, Granjeaud S, et al. (1999) Sensitivity issues in DNA array-based expression measurements and performance of nylon microarrays for small samples. Hum Mol Genet 8, 1715–1722

Boers GH, Smals AG, Trijbels FJ, Fowler B, Bakkeren JA, et al. (1985) Heterozygosity for homocystinuria in premature peripheral and cerebral occlusive arterial disease. N Engl J Med 313, 709–715

Brattstrom L, Wilcken DE, Ohrvik J, Brudin L (1998) Common methylenetetrahydrofolate reductase gene mutation leads to hyperhomocysteinemia but not to vascular disease: the result of a meta-analysis. Circulation 98, 2520–2526

Brown PO, Botstein D (1999) Exploring the new world of the genome with DNA microarrays. Nat Genet 21, 33–37

Chen Z, Karaplis AC, Ackerman SL, Pogribny IP, Melnyk S, et al. (2001) Mice deficient in methylenetetrahydrofolate reductase exhibit hyperhomocysteinemia and decreased methylation capacity, with neuropathology and aortic lipid deposition. Hum Mol Genet 10, 433–443

Christensen B, Arbour L, Tran P, Leclerc D, Sabbaghian N et al. (1999) Genetic polymorphisms in methylenetetrahydrofolate reductase and methionine synthase, folate levels in red blood cells, and risk of neural tube defects. Am J Med Genet 84, 151–157

Clarke R, Smith AD, Jobst KA, Refsum H, Sutton L et al. (1998) Folate, vitamin B12, and serum total homocysteine levels in confirmed Alzheimer disease. Arch Neurol 55, 1449–1455

Cottrell S, Bicknell D, Kaklamanis L, Bodmer WF (1992) Molecular analysis of APC mutations in familial adenomatous polyposis and sporadic colon carcinomas. Lancet 340, 626–630

Dahl E, Koseki H, Balling R (1997) Pax genes and organogenesis. Bioessays 19, 755–765

Dominguez M, Brunner M, Hafen E, Basler K (1996) Sending and receiving the hedgehog signal: control by the Drosophila Gli protein Cubitus interruptus. Science 272, 1621–1625

Duggan DJ, Bittner M, Chen Y, Meltzer P, Trent JM (1999) Expression profiling using cDNA microarrays. Nat Genet 21, 10–14

Eisen MB, Spellman PT, Brown PO, Botstein D (1998) Cluster analysis and display of genome-wide expression patterns. Proc Natl Acad Sci USA 95, 14863–14868

Farese RV Jr, Herz J (1998) Cholesterol metabolism and embryogenesis. Trends Genet 14, 115–120

Fenech M (2001) The role of folic acid and vitamin B12 in genomic stability of human cells. Mutat Res 475, 57–67

Finkelstein JD (1990) Methionine metabolism in mammals. J Nutr Biochem 1, 228–237

Fleming A, Copp AJ (1998) Embryonic folate metabolism and mouse neural tube defects. Science 280, 2107–2109

Fodde R, Kuipers J, Rosenberg C, Smits R, Kielman M et al. (2001) Mutations in the APC tumour suppressor gene cause chromosomal instability. Nat Cell Biol 3, 433–438

Gilfix BM, Blank DW, Rosenblatt DS (1997) Novel reductant for determination of total plasma homocysteine. Clin Chem 43, 687–688

Goodrich LV, Johnson RL, Milenkovic L, McMahon JA, Scott MP (1996) Conservation of the hedgehog/patched signaling pathway from flies to mice: induction of a mouse patched gene by hedgehog. Genes Dev 10, 301–312

Gorlin RJ (1987) Nevoid basal-cell carcinoma syndrome. Medicine (Baltimore) 66, 98–113

Goyette P, Christensen B, Rosenblatt DS, Rozen R (1996) Severe and mild mutations in cis for the methylenetetrahydrofolate reductase (MTHFR) gene, and description of five novel mutations in MTHFR. Am J Hum Genet 59, 1268–1275

Gress TM, Hoheisel JD, Lennon GG, Zehetner G, Lehrach H (1992) Hybridization fingerprinting of high-density cDNA-library arrays with cDNA pools derived from whole tissues. Mamm Genome 3, 609–619

Gulati S, Baker P, Li YN, Fowler B, Kruger W, et al. (1996) Defects in human methionine synthase in cblG patients. Hum Mol Genet 5, 1859–1865

Hankey GJ, Eikelboom JW (2000) Homocysteine and vascular disease. Lancet 354, 407–413

Harris MJ, Juriloff DM (1999) Mini-review: toward understanding mechanisms of genetic neural tube defects in mice. Teratology 60, 292–305

International Genome Sequencing Consortium (2001) Initial sequencing and analysis of the human genome. Nature 409, 860–921

Janne PA, Mayer RJ (2000) Chemoprevention of colorectal cancer. N Engl J Med 342, 1960–1968

Joosten E, Lesaffre E, Riezler R, Ghekiere V, Dereymaeker L, et al. (1997) Is metabolic evidence for vitamin B-12 and folate deficiency more frequent in elderly patients with Alzheimer's disease? J Gerontol A Biol Sci Med Sci 52, M76–M79

Kang SS, Wong PW, Zhou JM, Cook HY (1986) Total homocyst(e)ine in plasma and amniotic fluid of pregnant women. Metabolism 35, 889–891

Kang SS, Wong PW, Bock HG, Horwitz A, Grix A (1991) Intermediate hyperhomocysteinemia resulting from compound heterozygosity of methylenetetrahydrofolate reductase mutations. Am J Hum Genet 48, 546–551

Kang SS, Wong PW, Malinow MR (1992) Hyperhomocyst(e)inemia as a risk factor for occlusive vascular disease. Annu Rev Nutr 12, 279–298

Kanwar YS, Manaligod JR, Wong PW (1976) Morphologic studies in a patient with homocystinuria due to 5, 10- methylenetetrahydrofolate reductase deficiency. Pediatr Res 10, 598–609

Kaplan KB, Burds AA, Swedlow JR, Bekir SS, Sorger PK et al. (2001) A role for the adenomatous polyposis coli protein in chromosome segregation. Nat Cell Biol 3, 429–432

Kirke PN, Molloy AM, Daly LE, Burke H, Weir DG et al. (1993) Maternal plasma folate and vitamin B12 are independent risk factors for neural tube defects. Q J Med 86, 703–708

Kisliuk R (1999) Antifolate drugs in cancer therapy. In: *Anticancer Drug Development Guide.* N.J.: Humana Press, pp 13–36

Leclerc D, Campeau E, Goyette P, Adjalla CE, Christensen B, et al. (1996) Human methionine synthase: cDNA cloning and identification of mutations in patients of the cblG complementation group of folate/cobalamin disorders. Hum Mol Genet 5, 1867–1874

Leclerc D, Wilson A, Dumas R, Gafuik C, Song D et al. (1998) Cloning and mapping of a cDNA for methionine synthase reductase, a flavoprotein defective in patients with homocystinuria. Proc Natl Acad Sci USA 95, 3059–3064

Lopez AJ (1998) Alternative splicing of pre-mRNA: developmental consequences and mechanisms of regulation. Annu Rev Genet 32, 279–305

Malinow MR, Rajkovic A, Duell PB, Hess DL, Upson BM (1998) The relationship between maternal and neonatal umbilical cord plasma homocyst(e)ine suggests a potential role for maternal homocyst(e)ine in fetal metabolism. Am J Obstet Gynecol 178, 228–233

Mayer EL, Jacobsen DW, Robinson K (1996) Homocysteine and coronary atherosclerosis. J Am Coll Cardiol 27, 517–527

Mercer JG, Hoggard N, Williams LM, Lawrence CB, Hannah LT et al. (1996) Localization of leptin receptor mRNA and the long form splice variant (Ob-Rb) in mouse hypothalamus and adjacent brain regions by in situ hybridization. FEBS Lett 387, 113–116

Miller JW (1999) Homocysteine and Alzheimer's disease. Nutr Rev 57, 126–129

Mills JL, McPartlin JM, Kirke PN, Lee YJ, Conley MR et al. (1995) Homocysteine metabolism in pregnancies complicated by neural-tube defects. Lancet 345, 149–151

MRC Vitamin Study Research Group (1991) Prevention of neural tube defects: results of the Medical Research Council Vitamin Study. Lancet 338, 131–137

Mudd SH, Finkelstein JD, Irreverre F, Laster L (1964) Homocystinuria: an enzymatic defect. Science 143, 1443–1445

Mudd SH, Levy HL, Skraus JP (2001) Disorders of transsulfuration. In: Scriver CR, Beaudet AL, Sly WS, Valle D (eds) *The Metabolic Basis of Inherited Disease,* vol II, 8th edn. (New York: McGraw Hill), pp 2007–2056

Muller T, Werne B, Fowler B, Kuhn W (1999) Nigral endothelial dysfunction, homocysteine, and Parkinson's disease. Lancet 354, 126–127

Murone M, Rosenthal A, de Sauvage FJ (1999) Sonic hedgehog signaling by the patched-smoothened receptor complex. Curr Biol 9, 76–84

Ogawa H, Gomi T, Takusagawa F, Fujioka M (1998) Structure, function and physiological role of glycine N-methyltransferase. Int J Biochem Cell Biol 30, 13–26

Pietrzik K, Bronstrup A (1997) Causes and consequences of hyperhomocyst(e)inemia. Int J Vitam Nutr Res 67, 389–395

Rosenblatt DS, Fenton WA (2001) Inherited disorders of folate and cobalamin transport and metabolism. In: Scriver CR, Beaudet AL, Sly WS, Valle D (eds) *The Metabolic Basis of Inherited Disease,* vol III, 8th edn. (New York: McGraw Hill), pp 3897–3933

Song J, Medline A, Mason JB, Gallinger S, Kim YI (2000) Effects of dietary folate on intestinal tumorigenesis in the apcMin mouse. Cancer Res 60, 5434–5440

Stabler SP, Marcell PD, Podell ER, Allen RH, Lindenbaum J (1986) Assay of methylmalonic acid in the serum of patients with cobalamin deficiency using capillary gas chromatography-mass spectrometry. J Clin Invest 77, 1606–1612

Steegers-Theunissen RP, Boers GH, Trijbels FJ, Eskes TK (1991) Neural-tube defects and derangement of homocysteine metabolism. N Engl J Med 324, 199–200

Steegers-Theunissen RP, Wathen NC, Eskes TK, van Raaij-Selten B, Chard T (1997) Maternal and fetal levels of methionine and homocysteine in early human pregnancy. Br J Obstet Gynaecol 104, 20–24

Su LK, Kinzler KW, Vogelstein B, Preisinger AC, Moser AR et al. (1992) Multiple intestinal neoplasia caused by a mutation in the murine homolog of the APC gene. Science 256, 668–670

Swanson DA, Liu ML, Baker PJ, Garrett L, Stitzel M et al. (2001) Targeted disruption of the methionine synthase gene in mice. Mol Cell Biol 21, 1058–1065

Tamayo P, Slonim D, Mesirov J, Zhu Q, Kitareewan S et al. (1999) Interpreting patterns of gene expression with self-organizing maps: methods and application to hematopoietic differentiation. Proc Natl Acad Sci USA 96, 2907–2912

Tolner B, Roy K, Sirotnak FM (1997) Organization, structure and alternate splicing of the murine RFC-1 gene encoding a folate transporter. Gene 189, 1–7

Ubbink JB, Hayward, Vermaak WJ, Bissbort S (1991) Rapid high-performance liquid chromatographic assay for total homocysteine levels in human serum. J Chromatogr 565, 441–446

van der Put NM, Gabreels F, Stevens EM, Smeitink JA, Trijbels FJ, et al. (1998) A second common mutation in the methylenetetrahydrofolate reductase gene: an additional risk factor for neural-tube defects? Am J Hum Genet 62, 1044–1051

Venter JC et al. (2001) The sequence of the human genome. Science 291, 1304–1351

Watanabe M, Osada J, Aratani Y, Kluckman K, Reddick R et al. (1995) Mice deficient in cystathionine beta-synthase: animal models for mild and severe homocyst(e)inemia. Proc Natl Acad Sci USA 92, 1585–1589

Welch GN, Loscalzo J (1998) Homocysteine and atherothrombosis. N Engl J Med 338, 1042–1050

Yi P, Melnyk S, Pogribna M, Pogribny IP, Hine RJ, et al. (2000) Increase in plasma homocysteine associated with parallel increases in plasma S-adenosylhomocysteine and lymphocyte DNA hypomethylation. J Biol Chem 275, 29318–29323